Ref.TH.1796-CERN

POLARIZABILITY CONTRIBUTION TO THE ENERGY LEVELS OF THE MUONIC HELIUM $(\mu^4He)^+$

J. Bernabeu
University of Barcelona
and
CERN - Geneva

and

C. Jarlskog
University of Lund
and
CERN - Geneva

A B S T R A C T

An experiment measuring the 2s-2p separation in the ion $(\mu^4He)^+$ is in progress at CERN. Comparison of the outcome of this experiment with the prediction of the quantum electrodynamics requires the knowledge of the hadronic correction due to the two-photon exchange mechanism. Therefore, we have calculated the correction to the energy levels of the ion $(\mu^4He)^+$ due to this mechanism. The hadronic contribution to the 2s-2p separation is found to be ~16 Å which is about three times larger than the expected experimental uncertainty.

Ref.TH.1796-CERN
22 December 1973

1. INTRODUCTION

A beautiful and precise measurement of the wavelength of the radiation 2S-2P in the ionic system $(\mu^4He)^+$ is in its phase of data analysis[1]. The comparison of the result of this experiment with the theory of QED is sensitive to the finite size effect calculated by Campani[2], and the polarizability correction due to the virtual inelastic excitations of ^{4}He. If the field created by the muon is treated as static, the corresponding energy shift is expected to be[3]

$$\Delta E_{n\ell} = -\left(\frac{e^2}{4\pi}\right)\frac{1}{2}\,\alpha_{He}\,\langle r^{-4}\rangle_{n\ell} \tag{1}$$

with α_{He} the electric polarizability of ^{4}He. With $\alpha = 0.07$ fm^3 which is the value found from forward dispersion relations using the sum rules of Quarati[4], and an effective cut-off for the S-state of the order $R \sim 2$ fm, we obtain an estimate for the polarizability correction to the 2S-2P energy difference $\Delta E \sim -6 \times 10^{-3}$ eV, which in the usual units in the literature corresponds to $\sim 0.04\ \alpha^2$ Ry. This is nearly a magnitude larger than the expected precision of the experiment. It is therefore necessary to study this correction carefully.

In a recent study by the authors[5], it was shown that the classical approximation for the muons, while giving the correct order of magnitude, is not accurate enough for a quantitative comparison with experiment in S-states. Furthermore, the effective cut-off parameter R is a fictitious quantity and does not appear in a "rigorous" formulation of the problem. In this paper we deal with this polarizability correction, corresponding to the two-photon exchange contribution with virtual inelastic excitations of ^{4}He.

In Section 2, the expression for the energy shift is derived for a hydrogen-like atom. We find that the scattering approximation in which the momentum of the lepton in the atomic orbit is neglected as compared to its mass, is sufficiently good for our purposes. This gives rise to an effective short-range (compared to one-photon exchange) interaction, and therefore the square of the wave function at the origin appears naturally as a factor in the expression for the energy shift. Specializing to helium, the energy shift involves structure functions occurring in the forward virtual Compton scattering on ^{4}He. In Section 3, from dispersion relations for these structure functions, we can express the energy shift in terms of quantities measurable in inelastic electron scattering on ^{4}He.

In Section 4, the input used in our calculation is discussed and compared with the available experimental data. We find that the data is too scant to allow an experimental determination of the structure functions. Fortunately, the region of low $(-q^2)$ dominates (q^2 is the mass of the virtual photon squared). In this region the structure functions can be extrapolated from the point $-q^2 = 0$

corresponding to real photons. For large $-q^2$ (i.e. $-q^2 \gtrsim 3\ fm^{-2}$) the structure functions are those of the quasi-elastic scattering. In the region in between, the structure functions are hard to determine because of binding energy and exclusion effects. Fortunately, we find that the model-dependent structure functions determined by us give an "effective" q^2 distribution consistent with that of a natural smooth interpolation between the regions of small and large $-q^2$. Our results and conclusions are given in Section 5. The main outcome of this study is that the polarizability contribution to the Lamb shift of the muonic helium is significant and must be included in quantitative comparisons. For the ordinary helium ion $(eHe)^+$, however, the effect is completely negligible.

2. TWO-PHOTON EXCHANGE CONTRIBUTION

In this section, the formalism for calculating the polarizability contribution to the energy levels of a hydrogen-like atom, especially $(\mu^4He)^+$, is given.

We begin by considering the process of elastic scattering of a muon (or electron) by ^{4}He. The relevant two-photon exchange diagrams are shown in Fig. 1, where $p(p')$ is the four momentum of the initial (final) lepton and $P(P')$ is that of the nucleus. We denote the T-matrix element corresponding to these diagrams by $T^{2\gamma}(p,p',P,P')$. The expression for this quantity involves a four-dimensional integration over the real part of the amplitudes occurring in the virtual Compton scattering on ^{4}He multiplied by propagators and kinematical factors. Going over to atomic physics, the lepton and the nucleus are bound by the wave function. Therefore the correction to the energy levels, apart from some over-all normalization factors, is obtained by multiplying the scattering T-matrix element $T^{2\gamma}(p,p',P,P')$ by appropriate initial and final wave functions in the momentum space and summing over all momenta. However, as is very often the case in atomic physics, the formalism can be considerably simplified by taking into account the fact that the nucleus is heavy and can be treated as if it were at rest (the correction due to the motion of the nucleus can be treated by itself). Furthermore, the velocity of the lepton in the atom is typically of the order $Z\alpha$, $\alpha = 1/137$. Therefore, for low Z, it is a very good approximation to neglect in $T^{2\gamma}$ the three-momenta $\bar{p}$ and $\bar{p}'$ as compared to the lepton mass. These approximations have two essential consequences, namely (i) the modulus squared of the wave function at the origin $|\psi_{n\ell}(0)|^2$ appears as a factor in the expression for the energy shift, and (ii) the aforementioned virtual Compton amplitude gets replaced by the forward virtual amplitude which has by far simpler structure.

The appearance of $|\psi_{n\ell}(0)|^2$ implies that the two-photon exchange mechanism (as compared to one-photon exchange) is a short-range interaction. Intuitively, this conclusion is reasonable since, classically, the longest range potential pertaining to this mechanism behaves as r^{-4}. In order to estimate the magnitude of the error possibly introduced, we calculate $\langle r^{-4}\rangle$ for the 2S atomic orbit and find that it is within 10% of the result obtained by factorizing $|\psi_{n\ell}(0)|^2$. Other effective potentials are of shorter range and therefore for them the approximation above gets better.

These approximations give the following expression for the energy shift $\Delta E_{n\ell}$

$$\Delta E_{n\ell} = \frac{-ie^4}{2mM}\,|\psi_{n\ell}(0)|^2 \int \frac{d^4q}{(2\pi)^4}\,\frac{T_{\mu\rho}L^{\mu\rho}}{(q^2)^2(q^2-2m\nu)}\,. \tag{2}$$

Here m(M) is the mass of the lepton (nucleus) and $\psi_{n\ell}(0)$ denotes the wave function at the origin. $L^{\mu\rho}$ is the leptonic tensor given by

$$L^{\mu\rho} = p^\mu(p^\rho - q^\rho) + p^\rho(p^\mu - q^\mu) + g^{\mu\nu} m\nu \tag{3}$$

where $\nu = q_0$ and $p^\mu = (m,\vec{0})$. The hadronic tensor $T_{\mu\rho}$, coming from the lower part of the diagrams in Fig. 1, is the spin averaged forward virtual Compton amplitude for scattering on the nucleus (in our case ^{4}He).

We write the usual invariant decomposition of this tensor in the form

$$T_{\mu\rho} = -\left(g_{\mu\rho} - \frac{q_\mu q_\rho}{q^2}\right)T_1(\nu,q^2) + \left(P_\mu - \frac{M\nu}{q^2}q_\mu\right)\left(P_\rho - \frac{M\nu}{q^2}q_\rho\right)\frac{T_2(\nu,q^2)}{M^2} \tag{4}$$

with P^μ the four momentum of the nucleus. Further, we introduce the longitudinal amplitude defined by

$$T_L(\nu,q^2) = \left(1 - \frac{\nu^2}{q^2}\right)T_2(\nu,q^2) - T_1(\nu,q^2)\,. \tag{5}$$

In terms of $T_2(\nu,q^2)$ and $T_L(\nu,q^2)$, the expression for $\Delta E_{n\ell}$, Eq. (2) can be written in the form

$$\Delta E_{n\ell} = \frac{ie^4}{(2\pi)^4}\,\frac{m}{M}\,|\psi_{n\ell}(0)|^2 \int \frac{d^4q}{(q^2)^2}\,\frac{2\nu^2(1-\nu^2/q^2)T_2 - (q^2+2\nu^2)T_L}{(q^2)^2 - 4m^2\nu^2}\,. \tag{6}$$

To proceed further, we write unsubtracted dispersion relations for the amplitudes $T_2(\nu,q^2)$ and $T_L(\nu,q^2)$. This is reasonable in the nuclear case if we restrict ourselves to quasi-elastic excitations. Note, however, that the amplitude $T_1(\nu,q^2)$ needs a subtraction independently of the convergence of the dispersion integral because it must give the correct Thomson limit.

Introducing $W_i(\nu,q^2) = 1/2\pi \text{ Im } T_i(\nu,q^2)$, $i = 1, 2$, and L, and using the property $W_i(\nu,q^2) = -W_i(-\nu,q^2)$, we have for fixed q^2

$$T_L(\nu,q^2) = 4\int_0^\infty d\nu' \frac{\nu' W_L(\nu',q^2)}{\nu'^2-\nu^2} = T_L^P(\nu,q^2) + T_L^C(\nu,q^2), \tag{7}$$

$$T_2(\nu,q^2) = 4\int_0^\infty d\nu' \frac{\nu' W_2(\nu',q^2)}{\nu'^2-\nu^2} = T_2^P(\nu,q^2) + T_2^C(\nu,q^2) \tag{8}$$

where T_i^P and T_i^C refer to the pole and continuum contributions, respectively. For ^{4}He, continuum starts at $\nu = \nu_{th}(q^2)$, $\nu_{th}(q^2) = B - q^2/2M$ where B is the difference of binding energies of ^{4}He and ^{3}H.

The subtracted dispersion relation for $T_1(\nu,q^2)$ reads

$$T_1(\nu,q^2) = T_1(0,q^2) + 4\nu^2\int_0^\infty \frac{d\nu'}{\nu'} \frac{W_1(\nu',q^2)}{\nu'^2-\nu^2} = \tag{9}$$
$$= T_1(0,q^2) + T_1^P(\nu,q^2) + T_1^C(\nu,q^2).$$

3. APPLICATION TO ^{4}He

We consider the pole contributions occurring in the above expression. For a spin-zero target, as in our case, $W_1^P(\nu,q^2)$ vanishes identically. We find

$$T_1^P(\nu,q^2) = 0\,, \tag{10}$$

$$T_2^P(\nu,q^2) = \frac{-8M^2q^2}{(q^2)^2-4M^2\nu^2}\, Z^2|F(q^2)|^2, \tag{11}$$

$$T_L^P(\nu,q^2) = \frac{-8M^2q^2}{(q^2)^2-4M^2\nu^2}\, Z^2|F(q^2)|^2\left(1-\frac{q^2}{4M^2}\right), \tag{12}$$

where $F(q^2)$ is the electromagnetic form factor of ^{4}He. Using these relations and the definitions of T_i^C the subtraction constant is found to be

$$T_1(0,q^2) = -2Z^2|F(q^2)|^2 + 4\int_{\nu_{th}(q^2)}^\infty \frac{d\nu'}{\nu'}\left[W_1(\nu',q^2) + \frac{\nu'^2}{q^2}W_2(\nu',q^2)\right]. \tag{13}$$

In the limit $-q^2 \to 0$ the integral does not contribute and we find

$$\lim_{-q^2\to 0} T_1(0,q^2) = -2Z^2, \tag{14}$$

which, in our normalization, is the Thomson limit.

Next we consider the Born contribution to the amplitudes $T_i(\nu,q^2)$ the reason being that such a contribution with point-like form factor is already included in the iteration of the effective potential when pure quantum electrodynamical effects are calculated. Here, the diagrams with ^{4}He exchange, shown in Fig. 2a and 2b, are not gauge invariant. Adding the contact term (Fig. 2c), the total "Born contribution" becomes gauge invariant. Moreover, we find that the Born and pole contributions are identical. This result is due to spin of ^{4}He being zero, i.e. $T_1^P(\nu,q^2) = 0$. It does not hold for spin-½ targets[5].

From tensorial decomposition of $T_{\mu\rho}$ we find

$$\lim_{-q^2\to 0} \frac{\nu^2 T_2(\nu,q^2)}{-q^2} = \lim_{-q^2\to 0} T_1(\nu,q^2). \tag{15}$$

Taking now $\nu \to 0$ on both sides we have

$$\lim_{\nu\to 0}\ \lim_{-q^2\to 0} \frac{\nu^2 T_2(\nu,q^2)}{-q^2} = -2Z^2 + 2M\nu^2 \frac{(\alpha_{He}+\beta_{He})}{e^2/4\pi} \tag{16}$$

where $\alpha_{He} + \beta_{He}$ is the total polarizability of ^{4}He in real Compton scattering (see below). It is interesting to note that the Thomson limit is reproduced independent of the order in which we let $-q^2$ and ν go to zero, a result which is not valid for a spin-½ target due to the presence of the anomalous magnetic moment. Furthermore, we find that the electric polarizability of the target is related to the longitudinal amplitude. Specifically, it is proportional to the finite quantity

$$\lim_{-q^2\to 0} \frac{1}{2M} \frac{T_L^c(0,q^2)}{-q^2}.$$

Our formula for ΔE, expressed in terms of W_2 and W_L, reads

$$\Delta E_{n\ell} = \frac{-me^4}{M\pi^3} |\psi_{n\ell}(0)|^2 \int_0^\infty \frac{dt}{t^2} \int_0^{\sqrt{t}} d\xi \sqrt{t-\xi^2} \int_0^\infty \nu' d\nu' \times$$
$$\times \frac{[(t+2\xi^2)W_L - 2\xi^2(1-\xi^2/t)W_2]}{(\nu'^2+\xi^2)(t^2+4m^2\xi^2)} \tag{17}$$

where $W_i = W_i(\nu',-t)$, $t = -q^2$. In obtaining Eq. (17) we have performed a Wick rotation, the details of which are given in Ref. 5. Furthermore, as mentioned above we must subtract the point-like pole contribution to W's.

The integration over ξ can be easily performed, we find

$$\Delta E_{nl} = -2\left(\frac{e^2}{4\pi}\right)^2 \frac{|\psi_{nl}(0)|^2}{mM} \int_0^\infty \frac{dt}{t^2} \int_0^\infty \nu' d\nu' \left\{ C_L W_L(\nu',-t) + C_2 W_2(\nu',-t) \right\}, \tag{18}$$

$$C_L = C_L(\nu',t) = -2 - \frac{4m^2 t}{t^2 - 4m^2\nu'^2}\left[\left(1-\frac{t}{2m^2}\right)\sqrt{1+\frac{4m^2}{t}} - \left(1-2\frac{\nu'^2}{t}\right)\sqrt{1+\frac{t}{\nu'^2}}\right], \tag{18a}$$

$$C_2 = C_2(\nu',t) = 2\left\{ 3/2 + \frac{t}{4m^2} + \frac{\nu'^2}{t} - \frac{4m^2 t}{t^2-4m^2\nu'^2}\left[\frac{t\left(1+\frac{t}{4m^2}\right)}{4m^2}\sqrt{1+\frac{4m^2}{t}} - \frac{\nu'^2}{t}\left(1+\frac{\nu'^2}{t}\right)\sqrt{1+t/\nu'^2}\right]\right\}. \tag{18b}$$

We examine the integral in Eq. (18) in the limit $t \to 0$ and find

$$C_L W_L(\nu',-t) + C_2 W_2(\nu',-t) = \frac{2m\sqrt{t}}{\nu'^2} W_L(\nu',-t) - \frac{3t}{4\nu'^2} W_2(\nu',-t) + \mathcal{O}(t^2\sqrt{t}). \tag{19}$$

From Eq. (19) is seen that in the limit $t = -q^2 \to 0$ the dominant term $[\mathcal{O}(1/\sqrt{t})]$ in the integrand of Eq. (18) is proportional to the electric polarizability (α_{He}) of ^{4}He, and the next order term (order constant) is proportional to the sum of the electric and magnetic (β_{He}) polarizabilities as measured in real Compton scattering on ^{4}He where

$$\alpha = \frac{e^2}{4\pi}\frac{2}{M} \lim_{-q^2\to 0} \int_0^\infty \frac{d\nu}{\nu} \frac{W_L(\nu,q^2)}{-q^2}, \tag{20}$$

$$\alpha + \beta = \frac{e^2}{4\pi}\frac{2}{M} \lim_{-q^2\to 0} \int_0^\infty \frac{d\nu}{\nu} \frac{W_2(\nu,q^2)}{-q^2}. \tag{20a}$$

Fortunately, therefore, the leading terms in Eq. (18) are determined by the global properties of ^{4}He. For this nucleus one finds[4] $\beta_{He} \ll \alpha_{He}$ and $\alpha_{He} = 0.07$ fm^3.

4. INELASTIC STRUCTURE FUNCTIONS

The structure functions $W_2(\nu,q^2)$ and $W_L(\nu,q^2)$ are quantities measurable in inelastic electron scattering on ^{4}He, for which the differential cross-section is given by the usual formula

$$\frac{d^2\sigma}{d|q^2|d\nu} = \frac{\pi\alpha^2 E'}{4E(q^2)^2}\left\{\cos^2\frac{\theta}{2}\, W_2(\nu,q^2) + 2\sin^2\frac{\theta}{2}\, W_1(\nu,q^2)\right\},$$

$$W_1(\nu,q^2) = (1-\nu^2/q^2)\, W_2(\nu,q^2) - W_L(\nu,q^2), \tag{21}$$

where $E(E')$ is the energy of the incoming (outgoing) electron and θ is the scattering angle. Further $\nu = E - E'$, $\alpha = 1/137$, and $q^2 = -4EE' \sin^2 \theta/2$; the electron mass has been neglected.

Experiments have been performed by Frosch et al.[6] at different incoming energies and scattering angles. In Fig. 3 we show the region of the $\nu - q^2$ plane covered in these experiments. In this figure, the lines ^{4}He and p + ^{3}H correspond to the elastic scattering and the threshold for e(^{4}He, p^{3}H)e respectively. Data were taken along the lines designated by the scattering angle (in degrees) and the incoming energy (in MeV).

In order to separate $W_2(\nu,q^2)$ and $W_L(\nu,q^2)$ a point in this plane should be touched by two or more lines. As is seen from this figure this is not the case and the data do not permit the separation of the structure functions.

In Ref. 6 an analysis of the electrodisintegration spectrum was made under the assumption that it is nearly symmetric in shape and achieves its maximum value in ν at a position approximately 20 MeV above that of a free nucleon elastic peak. An estimate was made of the total disintegration cross-section $d\sigma/d\Omega$ and the reduction factor f, defined by

$$\frac{d\sigma}{d\Omega} = f\left\{2\left.\frac{d\sigma}{d\Omega}\right|_p + 2\left.\frac{d\sigma}{d\Omega}\right|_n\right\} \tag{22}$$

was determined. Here $d\sigma/d\Omega|_{p,n}$ are the differential cross-sections for scattering on protons and neutrons.

From these facts we shall take the ν distribution, at q^2 fixed, to be peaked around $\nu_{qel} = S + (-q^2/2M_n)$, where $S \approx 20$ MeV and M_n the nucleon mass. We define $W_2(q^2)$ and $W_L(q^2)$ using

$$W_i(\nu,q^2) = \delta\left(\nu - S + \frac{q^2}{2M_n}\right) M\, W_i(q^2), \quad i = 2, L \tag{23}$$

and they will be determined from the closure sum rules for quasi-elastic scattering. In that approach, binding energy effects are represented kinematically by the location of the peak (shown in Fig. 3 by the broken line) and dynamically by the Fermi motion of the internal nucleon, which contributes as an effective operator in the matrix element of the function $W_2(q^2)$. This is not surprising because it is due to this effect that photodisintegration exists in this description and we know that it is the function $W_2(\nu,q^2)/(-q^2)$ which survives in the limit of real photons. The exclusion principle effects are represented by the correlation functions which appear in the expectation values of two-body operators when closure is used (see, for example, Ref. 7). The calculation of $W_i(q^2)$ has been performed using the method worked out by Czyz et al.[8]. The radial matrix elements have been obtained using harmonic oscillator wave functions.

From Eqs. (20) and (23) the relevant quantities, for $-q^2 \to 0$, are

$$\alpha+\beta = \frac{e^2}{4\pi}\,\frac{2}{S}\lim_{-q^2\to 0}\frac{W_2(q^2)}{-q^2}$$
$$\alpha = \frac{e^2}{4\pi}\,\frac{2}{S}\lim_{-q^2\to 0}\frac{W_L(q^2)}{-q^2} \tag{24}$$

and thus we adjust the parameters appearing in $W_i(q^2)$, when applied to small values of $-q^2$, to reproduce $\alpha + \beta$ and α in Eqs. (24). However, if $-q^2 \gtrsim 2M_n S \approx 1\ \mathrm{fm}^{-2}$, the effects of the binding energy are expected to be negligible and the scattering is taken to be quasi-elastic only modified by the exclusion effects. Then α and β play no role and we take the oscillator parameter as determined in elastic scattering[6]. If $-q^2 \gtrsim 3\ \mathrm{fm}^{-2}$, nuclear structure effects disappear and the scattering is completely quasi-elastic.

We compare the reduction factor f obtained by us, following the prescriptions indicated above, with the "experimental estimate" of Ref. 6. The results are given in Table 1, where ν and $-q^2$ are the values of these variables at the quasi-elastic peak for a given incoming energy and scattering angle. We consider that the agreement for the values of f is sufficient, in view of the small sensitivity of the precise values of W_L and W_2 in that region for our polarizability correction. This will be manifest immediately below.

5. RESULTS AND CONCLUSIONS

We substitute our results above in the expression for the energy shift, Eq. (19). In order to see clearly the important region of integration, it is suitable to introduce the variable $v = \sqrt{t}/(\gamma + \sqrt{t})$, $\gamma = m/2$, m being again the lepton mass and $t = -q^2$. We find

$$\Delta E_{n\ell} = \frac{1}{2}\,\frac{e^2}{4\pi}\,\alpha_{He}\,|\psi_{n\ell}(0)|^2\, 4m\int_0^1 dv\, F(v), \tag{25}$$

$$F(v) = \frac{e^2}{4\pi} \frac{8}{m^3\alpha} \frac{1-v}{v^3} \frac{\nu_{qel}}{m} \left\{ C_L W_L + C_2 W_2 \right\} . \qquad (26)$$

Here $C_i = C_i(\nu_{qel}, t)$, $\nu_{qel} = S - t/2M_n$, and $W_i = W_i(q^2)$ [see Eqs. (18a), (18b), and (23)]. The function F(v) is shown in Fig. 4. We can distinguish between three different regions. The zone from v = 0 up to the first vertical arrow corresponds to the region in which the extrapolation from the real photons [see Eq. (19)] is very good. Here the

$$\lim_{v \to 0} F(v) = \lim_{v \to 0} \frac{1}{(1-v)^2} ,$$

i.e. if we extrapolate only the most dominant term corresponding to the first term in the right-hand side of Eq. (19), the result diverges badly. The inclusion of the second term in this equation removes this divergence and gives the shape depicted in Fig. 4. In the region beyond the second vertical arrow the scattering is completely quasi-elastic. The "critical" region, in which the structure effects are important, is situated between the two arrows and, as can be seen, we obtain a smooth distribution between these arrows.

Performing a numerical integration we find $\int_0^1 dv\, F(v) = 1.5$ which substituted above gives $\Delta E_{2S} = -3.1 \times 10^{-3}$ eV. Clearly $\Delta E_{2P} = 0$. The separation of the levels 2P-2S is therefore increased by an amount $|\Delta E| = 0.021\ \alpha^2$ Ry. This corresponds to a correction to the theoretical wavelength λ by the amount

$$\Delta\lambda = -\lambda^2 \frac{|\Delta E|}{2\pi} = -16\ \text{Å} .$$

As compared to the expected experimental accuracy (∿ 5 Å) our correction is significant.

Comparing our result with that of classical estimate [see after Eq. (1)], we see that our correction is about half as large in magnitude. It is known[10] that for electrons the classical approximation overestimates the polarizability correction by about two orders of magnitude. For muons, in the case of lepton-neutron scattering, we found[5] the classical estimate to be about twice as large in magnitude as the relativistic result which is quite similar to the result obtained here. Also, an earlier semiclassical calculation[11] gives $\Delta E_{2S} = -1.7 \times 10^6$ MHz which is again about twice as large in magnitude as our result.

The solid lines in Fig. 5 give the dependence of the wavelength on the $\langle r^2 \rangle^{\frac{1}{2}}$ of $(\mu^4He)^+$ as obtained by Campani[2]. The most accurate value of $\langle r^2 \rangle^{\frac{1}{2}}$, as measured[9] in electron scattering is 0.63 ± 0.04 fm. In this figure the ordinate to the right (left) is relevant to $2S_{1/2} - 2P_{3/2}$ $(2S_{1/2} - 2P_{1/2})$ transition. Including polarizability correction we obtain the dashed lines.

It is interesting to note that generally the comparison between theory and experiments in quantum electrodynamics (see, for example, Ref. 12) does not, in the present precision level, involve the hadronic corrections. However, for muonic and exotic atoms hadronic effects may become relevant. In the case considered by us clearly this is the case.

Acknowledgements

We wish to thank Drs. G. Carboni, T.E.O. Ericson and E. Zavattini for several enlightening discussions and the CERN Theoretical Study Division for the hospitality extended to us. One of us (J.B.) is indebted to GIFT for financial support during the early stages of this work.

REFERENCES

1) E. Zavattini, private communication.

2) E. Campani, Nuovo Cimento Letters 4, 982 (1970).

3) T.E.O. Ericson and J. Hüfner, Nuclear Phys. B47, 205 (1972).

4) P. Quarati, Nuclear Phys. A115, 651 (1968).

5) J. Bernabeu and C. Jarlskog, Nuclear Phys. B60, 347 (1973).

6) R.F. Frosch, R.E. Rand, H. Crannell, J.S. McCarthy, L.R. Suelzle and M.R. Yearian, Nuclear Phys. A110, 657 (1968).

7) J. Bernabeu, Nuclear Phys. B49, 186 (1972).

8) W. Czyz, L. Leśniak and A. Małecki, Ann. Phys. 42, 119 (1967).

9) W. Erich, H. Frank, D. Haas and H. Prange, Z. Phys. 209, 208 (1968).

10) L.S. Brown and A.M. Harun-ar-Rashid, Phys. Letters 42 B, 111 (1972).

11) C. Joachin, Nuclear Phys. 25, 317 (1961).

12) B.E. Lautrup, A. Peterman and E. de Rafael, Phys. Letters 3 C, 193 (1972).

Table 1

E (MeV)	θ (degrees)	ν (MeV)	$-q^2$ fm^{-2}	f^{-1}_{th}	f^{-1}_{exp}
169	39.7	26	0.29	14	16
199	45.0	30	0.50	7.8	12
199	60.0	37	0.83	4.6	4.9
199	75.0	44	1.2	3.1	3.9
199	90.0	51	1.5	1.4	1.6
399	45.0	62	2.0	1.3	1.5
399	50.0	70	2.4	1.2	1.2
399	60.0	86	3.2	1.1	1.1

Figure captions

Fig. 1a, 1b : Two-photon exchange diagrams for lepton-helium scattering.

Fig. 2a, 2b : Two-photon exchange "Born contribution".

Fig. 3 : The region of q^2-ν plane covered by experiment in Ref. 6 (see Section 4).

Fig. 4 : The function F(v) introduced in Section 5.

Fig. 5 : The theoretical wavelength of the $2S_{1/2}$-$2P_{1/2}$ and $2S_{1/2}$-$2P_{3/2}$ separations as a function of $\langle r^2\rangle^{\frac{1}{2}}$ of ^{4}He. The solid (dashed) lines correspond to the prediction without (with) the polarizability contribution.

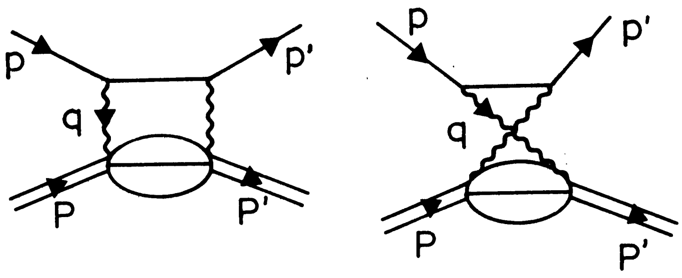

Fig. 1

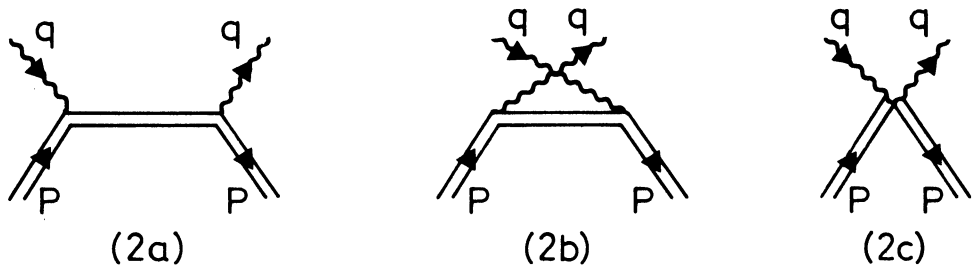

Fig. 2

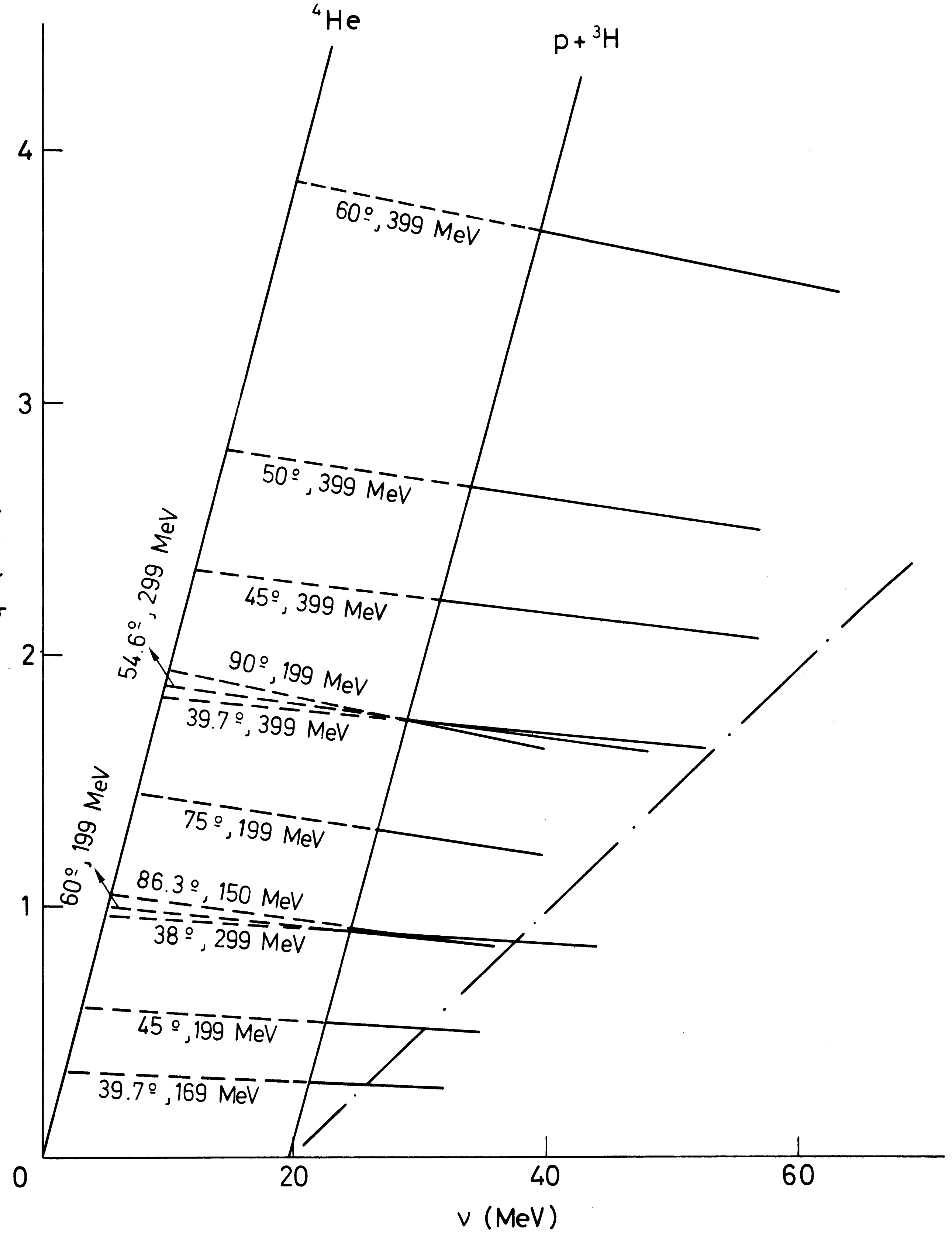

4He
p + 3H
60°, 399 MeV
50°, 399 MeV
45°, 399 MeV
54.6°, 299 MeV
90°, 199 MeV
39.7°, 399 MeV
75°, 199 MeV
60°, 199 MeV
86.3°, 150 MeV
38°, 299 MeV
45°, 199 MeV
39.7°, 169 MeV
-q2 (fm-2)
ν (MeV)
0
1
2
3
4
20
40
60

Fig. 3

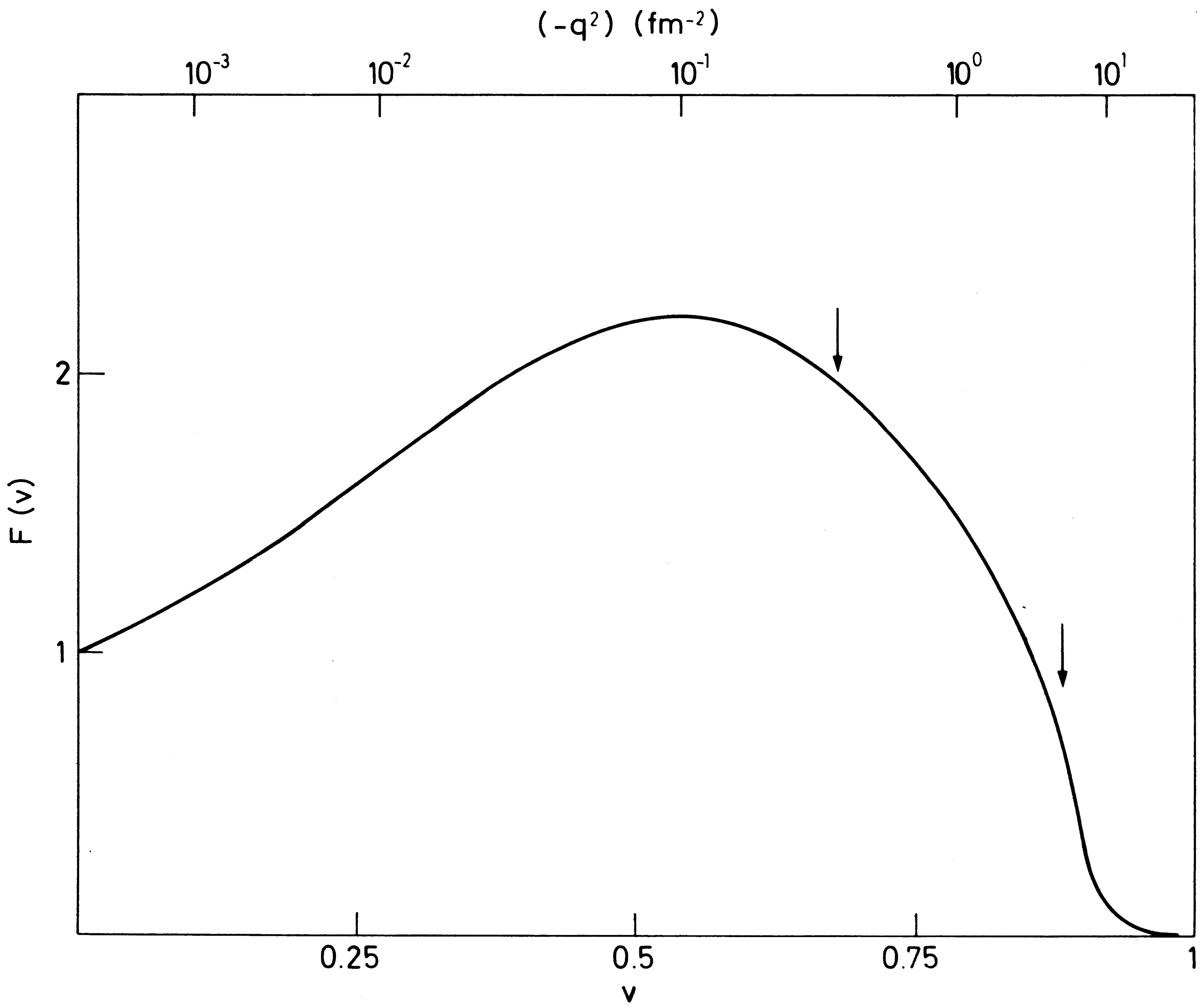

Fig. 4

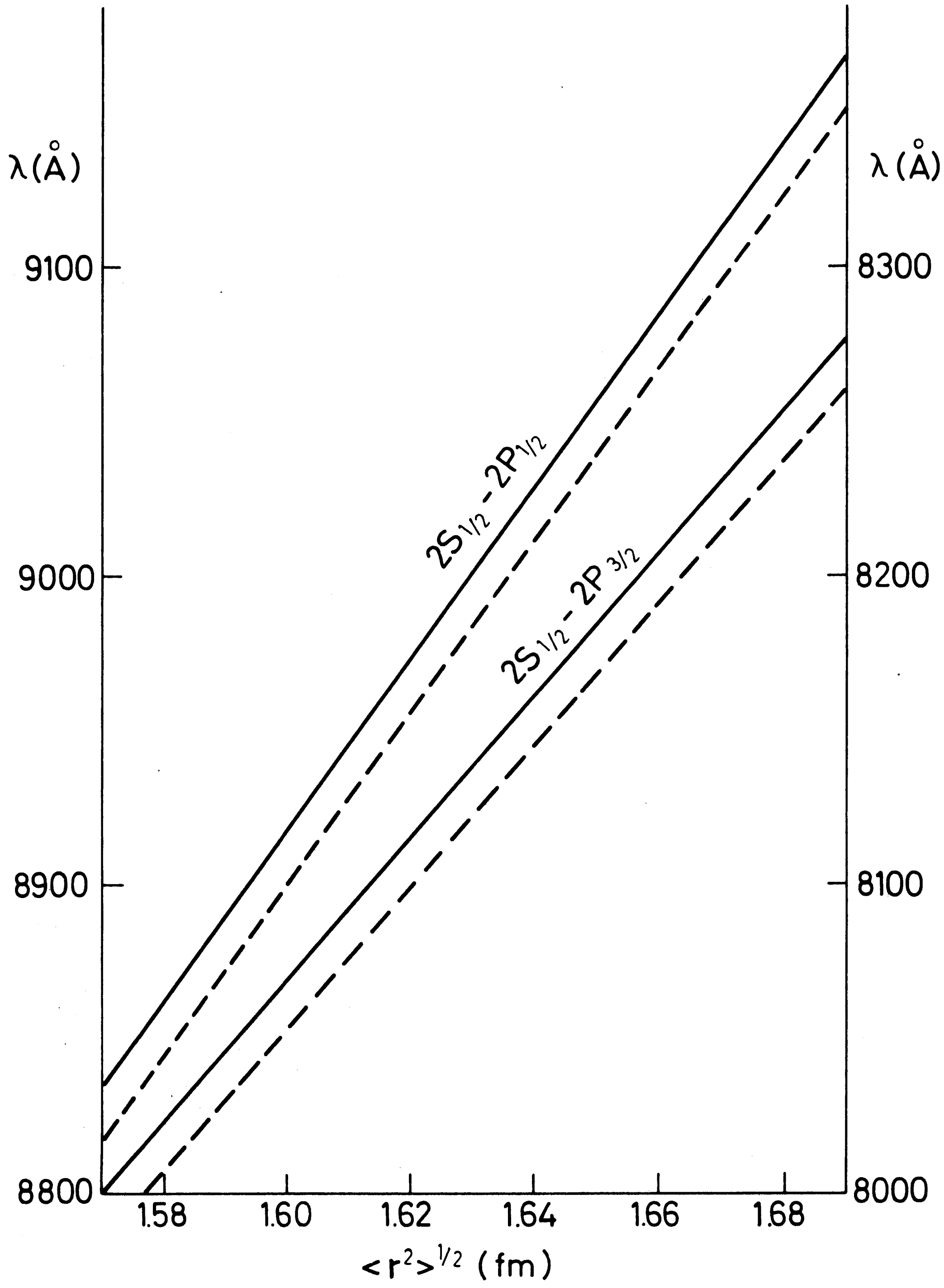
λ(Å)
λ(Å)
9100
9000
8900
8800
8300
8200
8100
8000
2S1/2 - 2P1/2
2S1/2 - 2P3/2
1.58
1.60
1.62
1.64
1.66
1.68
<r²>^1/2 (fm)

Fig. 5